Original Article

Clinicopathological and prognostic implications of vessels encapsulate tumor clusters with PD-L1 in intrahepatic cholangiocarcinoma patients

Ping Tao[1#], Lijie Ma[2#], Ruyi Xue[3#], Haijie Wang[1], Si Zhang[4]

[1]Department of Anatomy, Histology and Embryology, School of Basic Medical Sciences, [2]Department of Liver Surgery and Transplantation, Liver Cancer Institute, Zhongshan Hospital, and Key Laboratory of Carcinogenesis and Cancer Invasion (Ministry of Education), [3]Department of Gastroenterology and Hepatology, Shanghai Institute of Liver Diseases, Zhongshan Hospital, [4]Department of Biochemistry and Molecular Biology, School of Basic Medical Sciences, Fudan University, Shanghai 200032, China

[#]These authors contributed equally to this work.

Contributions: (I) Conception and design: S Zhang; (II) Administrative support: R Xue, L Ma, H Wang; (III) Provision of study materials or patients: P Tao; (IV) Collection and assembly of data: P Tao, L Ma; (V) Data analysis and interpretation: P Tao, L Ma; (VI) Manuscript writing: All authors; (VII) Final approval of manuscript: All authors.

Correspondence to: Si Zhang, PhD. Gene Research Center, Shanghai Medical College of Fudan University, 130 Dong-an Road, Xuhui District, Shanghai 200032, China. Email: zhangsi@fudan.edu.cn; Haijie Wang, PhD. Department of Anatomy, Histology and Embryology, School of Basic Medical Sciences, Fudan University, 130 Dong-an Road, Xuhui District, Shanghai 200032, China. Email: hjwang@shmu.edu.cn.

Background: Frequently abnormal vascularization and immunologic derangement have been uncovered in malignant tumors. In present research, we evaluated prognostic characteristic and clinicopathological features of vessels encapsulate tumor clusters (VETC) and the immune checkpoint molecule, programmed cell death-ligand 1 (PD-L1) in patients diagnosed as intrahepatic cholangiocarcinoma (ICC).

Methods: VETC and PD-L1 were investigated in two cohort enrolling 412 ICC patients. VETC and PD-L1 was easily detectable in whole slides and tissue microarray (TMA). Prognostic analysis was performed through Kaplan-Meier cures, log-rank tests and nomograms.

Results: VETC+ was significantly associated with aggressive tumor features. VETC+ predicted a significantly unfavorable survival and higher metastasis and recurrence rates. Furthermore, nomograms integrated by the combination of VETC and PD-L1, that heralded better prognostic value compared to previous staging systems.

Conclusions: Heterogeneous patterns of VETC phenotype and PD-L1 status were both illustrated to be an independent prognostic predictor for clinical outcomes. Therapies designed to target both vascularization and autoimmunity may open a novel direction for HCC. HCC should be replaced by ICC.

Keywords: Vessels encapsulate tumor clusters (VETC); PD-L1; nomogram; prognosis; intrahepatic cholangiocarcinoma (ICC)

Submitted Feb 20, 2020. Accepted for publication Mar 25, 2020.
doi: 10.21037/tcr.2020.04.11
View this article at: http://dx.doi.org/10.21037/tcr.2020.04.11

Introduction

Intrahepatic cholangiocarcinoma (ICC) ranks second and accounts 10–15% in primary liver cancers (1). Although ICC has made great progress in molecular basis, diagnosis and treatment, its morbidity and mortality are still steadily increasing worldwide (2). Currently, most ICC patients are diagnosed with advanced disease, as they are not eligible for complete surgical resection (3). Therefore, new models and biomarkers are urgently needed to stratify ICC patients based on their prognosis for better risk stratification and

comprehensive treatment.

Tumor metastasis is a multi-step and complex process that can be divided into local infiltration and intravascular perfusion (4). Intravascular perfusion is a process that relies on tumor cells entering the surrounding blood vessels, as angiogenic tumors are more likely to be perfused intravascularly (5). Therefore, the unique pattern of vascularization by tumor-associated angiogenesis and pathological capillary formation predicts rapid tumor diffusing and high recurrence rates (6). Remarkably, previous researched illustrated a novel pattern of vascularization, characterized by CD34 positive staining completely encapsulating tumor clusters, named VETC, was significant associated with higher metastasis and recurrence rates in hepatocellular carcinoma (HCC) (7). Furthermore, significantly benefit with the treatment of sorafenib was further uncovered in the presence of VETC than those absence in HCC patients (8). This novel pattern of vascularization, which is different from traditional capillaries, forming a spider web network and tumor islands (9). However, it remained unknown how this vascularization is formed in ICC. As the prognostic significance associated with VETC was unknown in ICC, these observations prompted us to consider that whether VETC affected angiogenesis in ICC.

The immune checkpoint index combined programmed death receptor-1 (PD-1) and programmed death ligand 1 (PD-L1) was treated as the main target of immunotargeted therapy in several malignant tumors with aberrant PD-L1 expression (10-12). In addition, elevated expression of PD-1/PD-L1 index was illustrated as survival predictor for HCC (13). Aberrant status of PD-1/PD-L1 discovered on tumor associated lymphocytes, endothelial cells and tumor cells, was defined as a signal of immune suppression (14). Previous researches indicated that elevated PD-L1 was found and further defined as an immune escape mechanism for occupational cholangiocarcinoma (15). However, due to the tumor heterogeneity and complex etiology, previous studies had indicated that PD-L1 was elevated and predicted dismal prognosis in ICC (16). Therefore, we evaluated the PD-L1 status in two independent cohorts enrolling 412 ICC cases from a single institution. As immune checkpoint blockade test with anti-PD-1 inhibitor was performed in several clinical trials, we confirmed that the drug resistance within anti-PD-1 inhibitor would be the majority challenge in ICC patients.

Five-year survival rate of advanced ICC is poorer than 5% due to poor efficacy of non-systemic treatment and chemotherapy drugs (17), and rare randomized trials of chemotherapy were launched in patients with advanced ICC (18). Previous research indicated that gemcitabine and platinum was defined as the first-line treatment for advanced cholangiocarcinoma. In addition, the treatment of gemcitabine combined with oxaliplatin and cetuximab, indicated a positive objective response rate of 63% in three cholangiocarcinoma patients (19). Nonetheless, the systemic therapeutic efficacy in ICC is far from satisfactory.

Whether the combination of immune checkpoint blockade with other types of therapies could improve anti-tumor efficacy in ICC, would be a leading challenge in the near future. Consistent with the previous studies in HCC, ICC also presented an elevated vascularization (20). Investigating this vascularization pattern was crucial, since combination therapy might produce better efficacy than monotherapy (21). Remarkably, previous research indicated that immune checkpoint blockade could enhance intra-tumor blood perfusion through the vascular normalization in both preclinical models of colorectal and breast cancers (22). In addition, the combination of anti-PD-1 and anti-VEGFR-2 inhibitors could evaluate the normal vascularization and enhance the anti-tumor efficacy in various malignancies (23). Nonetheless, the specific role remained unknown in the combination of immune checkpoint blockade with anti-VEGF/R therapy in ICC.

According to this, we assumed that VETC presenting and elevated PD-L1 expression could be defined as survival predictors for ICC. In addition, VETC presenting and elevated PD-L1 expression were significantly correlated with aggressive tumor features and independently associated with dismal clinical results, which could effectively stratify patients. Furthermore, we established an integrated nomogram with VETC/PD-L1 index for a more accurate prognosis prediction for ICC.

Methods

Patients and study design

Four hundred and twelve patients performed partial hepatectomy and diagnosed as ICC from January 2005 to December 2015 at Zhongshan Hospital (Shanghai, China) were selected in present study, and randomly grouped into training cohort (n=214), validation cohort (n=108) and external validation cohort (n=90). The study was approved by research ethics committee board of Zhongshan Hospital, Fudan University (No.: y2017-179). Written informed consent was obtained from the patient for publication of this study and signed consent forms are kept in the medical

records library. Overall survival (OS) and time to relapse (TTR) were carried out as described previously based on our established guidelines (24).

IHC staining

Detailed construction protocol of tissue microarray (TMA) and immunohistochemistry (IHC) protocol were summarized and consistent with previous study (25). Briefly, after deparaffinization of paraffin-embedded sections, antigen recovery was operated using buffer citric acid (pH =6.0). Slides were incubated with primary antibody overnight at 4 ℃. Followed rewarming for 45 minutes and incubating with secondary antibody for 30 minutes, slides were stained with 3, 3'-diaminobenzidine solution and then visualized by hematoxylin. Detailed information of IHC reagents were summarized: CD34 (CD34, clone QBEnd/10, 1:200; Santa Cruz Bio-technology), PD-L1 (PD-L1, clone SP263, 1:200; Ventana).

Evaluation of immunohistochemical staining signals

For CD34 evaluation, immunoreactivity that is continuously arranged around the tumor cluster, and VETC$^+$ was evaluated semi-quantitatively and defined as CD34 positive area ≥55%.

For PD-L1 evaluation, three representative images were obtained through Leica DM IRE2 microscope combined with Leica CCD camera DFC420. The combination of intensity and area of positive PD-L1 staining were calculated as the PD-L1 density.

Statistical analysis

IBM SPSS Statistics (Version 26) and R software were applied in the statistical analysis. Related transcriptome sequencing data of pan-cancer and cholangiocarcinoma (CHOL) cohorts were download from The Cancer Genome Atlas (TCGA) database. Continuous variables were compared though GraphPad Prism 7 software applying the Mann-Whitney U, χ^2, and Fisher's exact tests, respectively. Kaplan-Meier and log-rank test were used for OS and TTR evaluation. Cox regression analysis was performed for univariate and multivariate analyzing. Nomogram models were constructed by "Rms" package, and the Harrell's concordance index (C-index) was used for evaluating the discrimination performance of nomograms. All P values <0.05 were defined as statistical significant.

Results

Clinical features of selected ICC patients

The clinicopathological features of 412 ICC patients enrolled in training cohort, validation cohort and external validation cohorts were summarized in *Table 1*. Briefly, a strong HBV infection predominance was observed (60.3%, 64.8% and 77.8%). Most of ICC cases were Child-Pugh stage A (95.8%, 98.1% and 72.2%), and single tumor accounted to 78.5%, 70.4% and 76.7%, respectively. Tumor diagnosed as poorly differentiated of ICC (Edmondson grade III-IV) were accounted for 37.9%, 40.7% and 30%, respectively. The cumulative 1-, 3-, and 5-year OS rates were 76%, 46%, and 36% for training cohort. For validation cohort, the cumulative 1-, 3-, and 5-year OS rates were 78%, 44% and 34%, respectively. Additionally, the cumulative 1- and 3-year OS rates were 77%, 43% for external validation cohort. One hundred and one (47.2%), 63 (58.3%) and 38 (42.2%) occurred tumor recurrence within 2 years after surgery (early recurrence), 29 (13.5%), 7 (6.5%) and 38 (42.2%) after 24 months (late recurrence), and 84 (39.3%), 38 (35.2%) and 14 (15.6%) patients without recurrence for training, validation and external validation cohort, respectively.

VETC pattern and PD-L1 status in ICC patients

To identify VETC pattern and PD-L1 status in ICC, the transcriptomics profiles CD34 and PD-L1 were downloaded from FireBrowse database (26). Our finding indicated that the mRNA level of CD34 and PD-L1 were significant elevated in tumor area than those in non-tumor tissues in ICC (*Figure S1A,B*). According to the transcriptomics profiles of CD34 and PD-L1 in some tumors, down-regulation were also illustrated in other tumors. Hence, the specific position of VETC and PD-L1 should be evaluated in a specific role. Furthermore, positively and significantly correlation between the mRNA level of CD34 and PD-L1 in CHOL was uncovered by the TCGA database (pan-cancer cohort, R=0.13, P=1.7e-28; CHOL cohort, R=0.54, P=0.00012; *Figure S2A,B*).

VETC phenotype was evaluated by IHC in total 412 ICC using TMA. Interestingly, two distinct vascular patterns in ICC was observed: tumor associated vessels combined with discrete lumens (defined as classical capillary vessels), and tumor associated vessels which encapsulated tumor cluster (VETC pattern). ICC patients were divided into VETC$^+$ and VETC$^-$, according to the VETC pattern

Table 1 Baseline demographic, clinicopathological characteristics and phenotypical features of the whole ICC series (n=412)

Variables	Training cohort (n=214)	Validation cohort (n=108)	External validation cohort (n=90)
Clinical features			
Gender (male *vs.* female)	123/91	71/37	53/37
Age, median (range), years	58 [31–81]	58 [27–79]	64 [36–93]
HBV infection (negative *vs.* positive)	85/129	38/70	20/70
AFP (ng/mL) (<20 *vs.* ≥20)	193/21	93/15	80/10
CA-199 (U/mL) (<37 *vs.* ≥37)	103/111	60/48	47/43
Lymphonodus metastasis (absent *vs.* present)	177/37	89/19	62/28
TNM stage (I *vs.* II+III)	164/50	83/25	67/23
Child-Pugh stage (A *vs.* B)	205/9	106/2	65/25
General macroscopic			
Tumor number (single *vs.* multiple)	168/46	76/32	69/21
Tumor size (≤5 *vs.* >5)	91/123	54/54	33/57
Macrovascular invasion (absent *vs.* present)	181/33	95/13	75/15
General microscopic			
Liver cirrhosis (absent *vs.* present)	154/60	82/26	62/28
Microvascular invasion (absent *vs.* present)	181/33	95/13	75/15
Tumor encapsulation (complete *vs.* none)	21/193	18/90	19/71
Tumor differentiation (I+II *vs.* III+IV)	133/81	64/44	63/27
Follow-up			
Survival (no *vs.* yes)	61/153	40/68	67/23
Recurrence (no *vs.* yes)	84/130	38/70	14/76
Recurrence (≤2 *vs.* >2 years)	101/29	63/7	38/38

ICC, intrahepatic cholangiocarcinoma; CA-199, carbohydrate antigen 199; TNM, tumor-nodes-metastases.

(*Figure 1A*). Sequence slices further showed that VETC formed a network around a single ICC nodule, while capillaries indicated a discrete and disordered pattern. However, among 412 ICC tissues examined, 61.9% were VETC$^+$ cases (255/412). These findings indicated that VETC is a prevalent pattern of vascularization in ICC.

Meanwhile, IHC evaluation of PD-L1 was performed in the same cohorts. The expression and distribution patterns of PD-L1 were found mainly distributed in both tumor cytoplasm and cell membrane (*Figure 1B*). However, Heterogeneous PD-L1 status within intra-tumor from different cases were also investigated. Consistent with the mRNA expression in TCGA database, the comparison had showed that significantly elevated PD-L1 expression in ICC intra-tumor area was found than those in adjacent normal intrahepatic biliary tissues (*Figure 1B*). Consistent with previous study, PD-L1 status was classified as hyper-activated in 50% (206 of 412) of intra-tumor areas, but 19.9% (82 of 412) were defined as hyper-activated in paired normal areas.

Relationship of clinicopathological features with VETC and PD-L1

To further investigated the association between clinicopathological features and VETC and PD-L1 in ICC

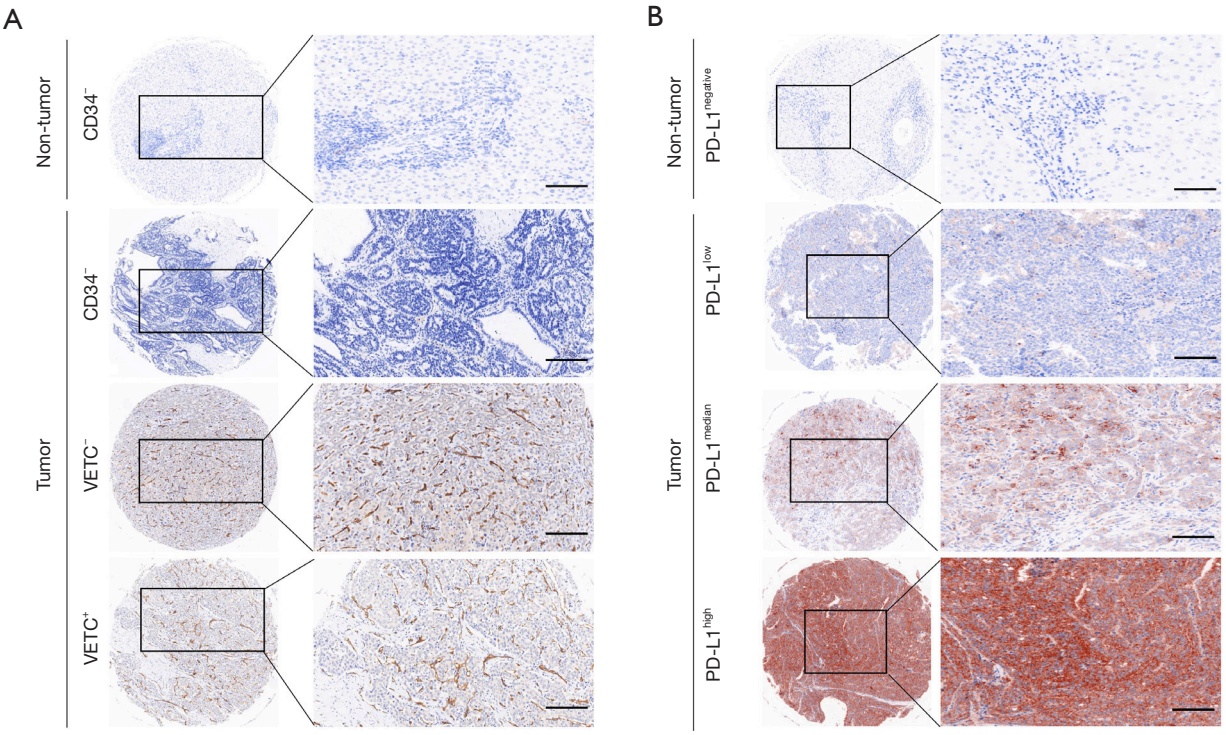

Figure 1 VETC pattern and PD-L1 expression in ICC. Representative images of VETC (A) pattern and PD-L1 (B) expression in ICC and adjacent non-tumor tissues. Up: adjacent non-tumor tissues. Bottom: different staining intensities in ICC. Magnification: ×200. VETC, vessels encapsulate tumor clusters; ICC, intrahepatic cholangiocarcinoma.

patients, training cohort were sub-grouped into absent (VETC$^-$) and present (VETC$^+$) groups, high (PD-L1^{high}) and low (PD-L1^{low}) expression groups, respectively.

Correlation analysis between clinicopathological features and VETC and PD-L1 were performed and summarized in *Table 2*, respectively. Remarkably, the presence of VETC$^+$ in intra-tumor area was significantly associated with more lymph node metastasis (P=0.017), more microvascular invasion (P=0.018), higher preoperative serum CA-199 level (P=0.021) and early postoperative recurrence (P=0.014). Likewise, elevated PD-L1 status in intra-tumor area was positively correlated with malignant characteristics in ICC, including susceptibility to HBV infection (P=0.035), more liver cirrhosis (P=0.017) and more tendentiousness of lymph node metastasis (P=0.024).

Similar results were also found in validation cohort and external independent cohorts. the presence of VETC$^+$ in intra-tumor area was significantly associated with higher preoperative serum CA-199 level (P=0.012), more microvascular invasion (P=0.003), more tendentiousness of lymph node metastasis (P=0.038) and early postoperative recurrence (P=0.037). Moreover, elevated PD-L1 status was significantly associated with more tendentiousness of lymph node metastasis (P=0.01) and elevated preoperative serum CA-199 level (P=0.028) (*Table 2*). Our findings presented that the presence of VETC and elevated PD-L1 status in ICC intra-tumor areas may signify the dismal clinical prognosis and malignant characteristics.

Prognostic values of VETC and PD-L1 in ICC

To further investigate the prognostic values, we assessed potential associations of VETC phenotype and PD-L1 status with patients' OS and TTR. In the training cohort, VETC$^+$ phenotype indicated significantly dismal OS (27 versus 72 months, P=0.0149; *Figure 2A*) and poorer TTR (14 versus 40.5 months, P=0.0022; *Figure 2B*) than those in VETC$^-$ patients. Similarly, in the validation cohort, VETC$^+$ patients showed both unfavorable survival and elevated recurrence (OS, P<0.0001; TTR, P=0.0002; *Figure S3A*). Consistently, in the external validation cohort, VETC$^+$ phenotype illustrated unfavorable prognosis than

Table 2 Correlation between VETC presenting and PD-L1 expression with clinicopathologic characteristics of the whole ICC series (n=412)

Characteristics	Training cohort (n=214)						Validation cohort (n=108)						External validation cohort (n=90)					
	VETC			PD-L1			VETC			PD-L1			VETC			PD-L1		
	Absent	Present	P	Low	High	P	Absent	Present	P	Low	High	P	Absent	Present	P	Low	High	P
Gender																		
Male	56	67	0.231	55	68	0.072	27	44	0.767	32	39	0.155	16	37	0.962	25	28	0.533
Female	34	57		52	39		13	24		22	15		11	26		15	22	
Age, year																		
≤58	54	63	0.182	65	52	0.074	19	33	0.917	22	30	0.123	16	38	0.925	25	29	0.665
>58	36	61		42	55		21	35		32	24		11	25		15	21	
HBsAg																		
Negative	50	81	0.147	73	58	0.035	18	20	0.101	32	6	<0.001	8	12	0.268	14	6	0.009
Positive	40	43		34	49		22	48		22	48		19	51		26	44	
AFP (ng/mL)																		
≤20	79	114	0.313	97	96	0.818	33	60	0.405	48	45	0.403	22	58	0.143	35	45	0.746
>20	11	10		10	11		7	8		6	9		5	5		5	5	
CA-199 (U/mL)																		
<37	35	68	0.021	49	54	0.494	16	44	0.012	32	28	0.438	8	34	0.007	24	23	0.186
≥37	55	56		58	53		24	24		22	26		18	29		16	27	
Liver cirrhosis																		
Absent	68	93	0.925	88	73	0.017	28	54	0.269	36	46	0.024	21	41	0.233	28	34	0.838
Present	22	31		19	34		12	14		18	8		6	22		12	16	
Tumor size (cm)																		
≤5	35	56	0.359	43	48	0.489	16	38	0.111	26	28	0.700	10	23	0.961	26	7	<0.001
>5	55	68		64	59		24	30		28	26		17	40		14	43	
Tumor number																		
Single	71	97	0.907	86	82	0.505	26	50	0.348	41	35	0.206	22	47	0.591	32	37	0.387
Multiple	19	27		21	25		14	18		13	19		5	16		18	13	
Microvascular invasion																		
Negative	70	111	0.018	92	89	0.570	30	65	0.003	48	47	0.767	18	57	0.005	36	39	0.161
Positive	20	13		15	18		10	3		6	7		9	6		4	11	
Tumor encapsulation																		
None	84	109	0.187	98	95	0.491	33	57	0.858	44	46	0.605	23	48	0.409	32	39	0.817
Complete	6	15		9	12		7	11		10	8		4	15		8	11	
Tumor differentiation																		
I+II	57	78	0.948	67	68	0.887	23	41	0.775	35	29	0.240	22	59	0.121	35	46	0.503
III+IV	33	46		40	39		17	27		19	25		5	4		5	4	

Table 2 (*continued*)

Table 2 (*continued*)

Characteristics	Training cohort (n=214)						Validation cohort (n=108)						External validation cohort (n=90)					
	VETC			PD-L1			VETC			PD-L1			VETC			PD-L1		
	Absent	Present	P	Low	High	P	Absent	Present	P	Low	High	P	Absent	Present	P	Low	High	P
Lymphonodus metastasis																		
Absent	82	98	0.017	96	84	0.024	29	60	0.038	48	41	0.076	24	42	0.037	20	42	0.0005
Present	8	26		11	23		11	8		6	3		3	21		20	8	
TNM stage																		
I	73	93	0.290	84	82	0.743	29	54	0.411	43	40	0.493	21	46	0.842	31	35	0.424
II+III	17	31		23	25		11	14		11	14		7	17		9	15	
Child-Pugh stage																		
0-A	86	119	0.882	105	100	0.088	39	67	>0.99	54	52	0.495	18	47	0.258	20	45	0.010
B-C	4	5		2	7		1	1		0	2		10	15		20	15	
Follow-up																		
Early recurrence (≤2 years)	38	65	0.014	52	51	0.667	39	24	0.037	31	32	0.996	9	29	0.009	10	28	0.091
Late recurrence (>2 years)	17	10		12	15		2	6		4	4		6	2		5	3	

*, P value <0.05 showed statistical significant. CA-199, carbohydrate antigen 199; TNM, tumor-nodes-metastases; VETC, vessels encapsulate tumor clusters; ICC, intrahepatic cholangiocarcinoma.

those in VETC$^-$ patients (OS, P=0.0004; TTR, P=0.0036; *Figure S3B*).

Furthermore, in the training cohort, PD-L1^{high} patients significantly indicated poorer OS and elevated recurrence than those in PD-L1^{low} (OS, P=0.0023; TTR, P=0.027; *Figure 2C,D*). Similarly, results were also found in the validation cohort (OS, P=0.0184; TTR, P=0.0306; *Figure S3C*) and external validation cohort (OS, P<0.001; TTR, P=0.109; *Figure S3D*).

Since a potential relationship of VETC and PD-L1 in tumor vascularization and a significantly correlation between CD34 and PD-L1 expression were found, we further constructed a VETC/PD-L1 index. According to this index, training cohort were sub-grouped into three distinct groups: (group I) VETC$^-$ and PD-L1^{low}; (group II) VETC$^+$ or PD-L1^{high}; and (group III) VETC$^+$ and PD-L1^{high}. Note-worthily, significant prognostic differences were illustrated within these three groups (OS, P<0.0001; TTR, P=0.0003; *Figure 2E,F*). The 5-year OS rates were 61%, 33.6% and 22.6% for group I, II, and III, respectively. Consistently, similar findings were also evaluated in the validation and external validation cohort (validation cohort, OS, P=0.0001, TTR, P<0.0001; *Figure S4A,B*; external validation cohort, OS, P<0.0001, TTR, P=0.004; *Figure S4C,D*). Furthermore, we investigated the univariate and multivariate analyses in both training cohort (*Table 3*) and validation cohort (*Table S1*), and VETC/PD-L1 index was illustrated as an independent predictor for both OS and early postoperative recurrence.

The construction and validation of the prognostic nomogram

Multivariable models were constructed by appropriate categories for all variables simultaneously. Based on our findings of both univariate and multivariate analysis, CA-199 level combined with lymph node metastasis and intra-tumoral VETC/PD-L1 index were subsequently used to build a corresponding nomogram for the prediction of OS (*Figure 3A,B*) at 3, 5 years after surgery. The total score

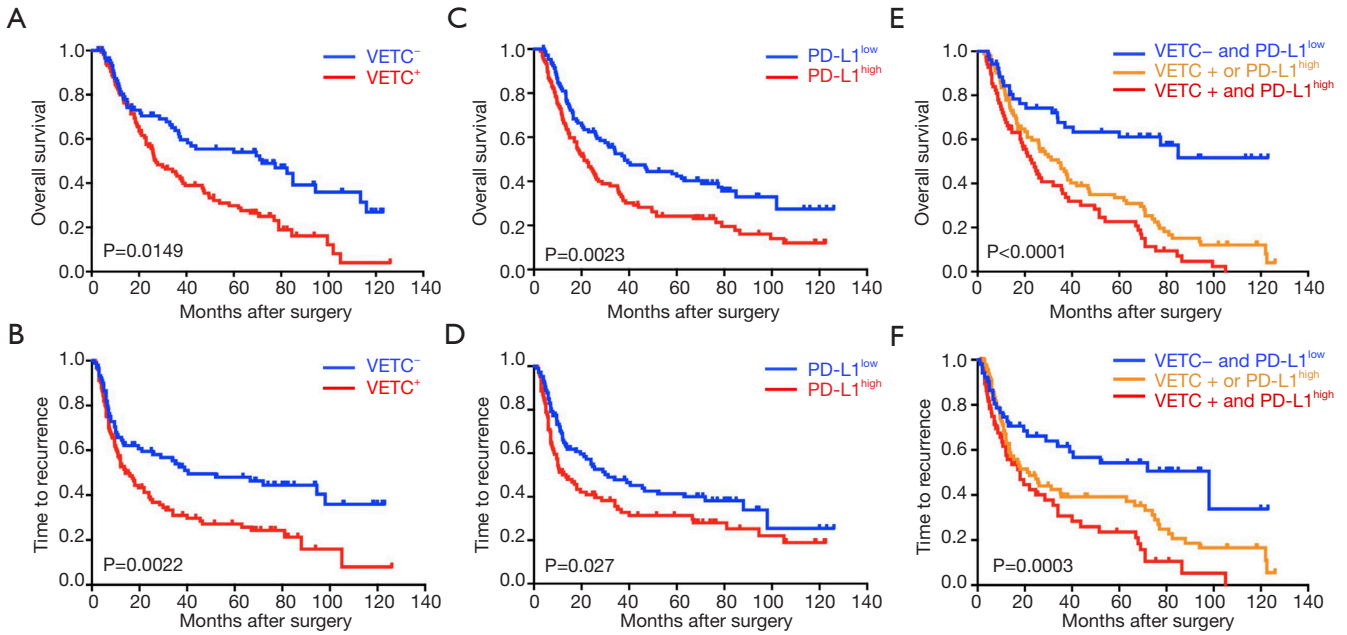

Figure 2 Clinical implications of VETC and PD-L1 in ICC. (A,B) Kaplan-Meier curves for OS and TTR based on VETC pattern in training cohort (n=214); (C,D) Kaplan-Meier curves for OS and TTR based on PD-L1 expression in training cohort (n=214); (E,F) Kaplan-Meier curves for OS and TTR based on combined VETC pattern and PD-L1 expression in training cohort (n=214). VETC, vessels encapsulate tumor clusters; ICC, intrahepatic cholangiocarcinoma; TTR, time to relapse; OS, overall survival.

of each nomogram indicates that the hierarchical prediction of patient prognosis is more accurate. For each nomogram, the predicted cumulative incidence of 3 or 5 years was compared to the observed actual incidence of 3 or 5 years, which showed a good calibration (*Figure 3C,D*). In addition, we found that the corresponding C-index for this specific OS nomogram was 0.718 [95% confidence interval (CI): 0.640–0.797] in the present study, which was better than those in TNM [the AJCC 7th edition Cancer Staging (27), C-index: 0.594, 95% CI: 0.55–0.638] (28), LCSGJ (C-index: 0.605, 95% CI: 0.561–0.649) (27), Nathan (C-index: 0.588, 95% CI: 0.543–0.633) (29) and Okabayashi staging systems (C-index: 0.594, 95% CI: 0.55–0.638) (30).

To validate the prognostic value in the validation cohort, nomograms constructed with similar features from training set were further used to predict the probability of OS (*Figure S5A,B*), with a corresponding C-index (0.691, 95% CI: 0.583–0.800) for this specific OS nomogram. The 3- and 5-year survival rates indicated by nomogram suitable well with this predicted model. Our findings indicated that a good concordance between predicted and observed survival probabilities were constructed through a favorable nomogram.

Discussion

ICC is an uncommon malignant tumor with a unfavorable prognosis due to an poor understanding of its molecular pathogenesis, the insufficient benefits of standard chemotherapy, and no optimal biomarkers used clinically to predict prognosis (31). Since the dismal prognosis in ICC, optimal predictors to sub-group ICC patients were significantly indeed.

It remained unknown that the vascularization pattern in intra-tumoral area could predict clinical benefit. VETC phenotype was defined as a novel peculiar vascular pattern with a common feature, that tumor nest were surrounded with dilated sinusoid-like structures (7). Previous studies indicated that VETC was not only tumor-riched in HCC, but also in follicular thyroid cancer and renal cell cancer (32). Recently, a multi-center cohort of HCC cases from different countries illustrated the universality of this vascularization pattern, and VETC⁺ phenotype was defined as an independent predictor for dismal OS and elevated recurrence (7). In addition, VETC pattern may present an effective transfer model through the promotion of tumor clusters releasing (33).

Furthermore, VETC phenotype may act as a novel

Table 3 Impact of clinical and pathological features on OS, TTR and early recurrence in training cohort (n=214)

Characteristics	OS (n=214)				TTR (n=214)				Early recurrence (n=214)			
	Univariable analysis		Multivariable analysis		Univariable analysis		Multivariable analysis		Univariable analysis		Multivariable analysis	
	HR (95% CI)	P	HR (95% CI)	P	HR (95% CI)	P	HR (95% CI)	P	HR (95% CI)	P	HR (95% CI)	P
Clinical features												
Gender (male *vs.* female)	1.005 (0.726–1.329)	0.974		NA	0.872 (0.615–1.235)	0.441		NA	0.973 (0.654–1.446)	0.891		NA
Age, median (range), years	1.128 (0.821–1.551)	0.457		NA	1.116 (0.789–1.577)	0.535		NA	1.100 (0.746–1.623)	0.631		NA
HBV infection (negative *vs.* positive)	0.847 (0.610–1.176)	0.321		NA	0.781 (0.545–1.119)	0.178		NA	0.805 (0.538–1.204)	0.290		NA
AFP (ng/mL) (<20 *vs.* ≥20)	0.956 (0.552–1.657)	0.872		NA	0.928 (0.500–1.722)	0.812		NA	0.942 (0.475–1.867)	0.864		NA
CA–199 (U/mL) (<37 *vs.* ≥37)	1.434 (1.0421.973)	0.027*	1.462 (1.057–2.022)	0.022*	1.084 (0.767–1.532)	0.647		NA	1.092 (0.742–1.608)	0.656		NA
Lymphonodus metastasis (absent *vs.* present)	2.220 (1.476–3.339)	<0.001*	1.564 (0.794–3.082)	0.196	1.874 (1.199–2.929)	0.006*	1.129 (0.516–2.470)	0.760	2.024 (1.261–3.248)	0.004*	1.258 (0.555–2.851)	0.582
TNM stage (I *vs.* II+III)	1.982 (1.383–2.842)	<0.001*	1.212 (0.660–2.225)	0.535	1.681 (1.130–2.501)	0.01*	1.491 (0.740–3.002)	0.264	1.865 (1.218–2.858)	0.004*	1.439 (0.689–3.004)	0.333
Child–Pugh stage (A *vs.* B)	0.653 (0.268–1.549)	0.350		NA	0.490 (0.130–1.286)	0.126		NA	0.347 (0.086–1.405)	0.138		NA
General macroscopic												
Tumor number (single *vs.* multiple)	1.437 (0.987–2.091)	0.058		NA	1.451 (0.963–2.186)	0.075		NA	1.363 (0.863–2.153)	0.185		NA
Tumor size (≤5 *vs.* >5)	1.328 (0.960–1.837)	0.087		NA	1.264 (0.889–1.795)	0.192		NA	1.431 (0.956–2.141)	0.081		NA
Macrovascular invasion (absent *vs.* present)	1.212 (0.783–1.875)	0.389		NA	1.660 (1.079–2.553)	0.021*	1.420 (0.914–2.205)	0.119	1.519 (0.932–2.475)	0.094		NA

Table 3 (*continued*)

Table 3 (*continued*)

Characteristics	OS (n=214)				TTR (n=214)				Early recurrence (n=214)			
	Univariable analysis		Multivariable analysis		Univariable analysis		Multivariable analysis		Univariable analysis		Multivariable analysis	
	HR (95% CI)	P	HR (95% CI)	P	HR (95% CI)	P	HR (95% CI)	P	HR (95% CI)	P	HR (95% CI)	P
General microscopic												
Liver cirrhosis (absent *vs.* present)	1.453 (1.021–2.07)	0.038*	1.209 (0.822–1.776)	0.335	1.123 (0.750–1.682)	0.574		NA	1.212 (0.781–1.881)	0.391		NA
Tumor encapsulation (complete *vs.* none)	1.578 (0.891–2.795)	0.118		NA	2.487 (1.212–5.104)	0.013*	2.556 (1.205–5.420)	0.014*	2.722 (1.108–6.691)	0.029*	2.747 (1.114–6.772)	0.028*
Differentiation (I/II *vs.* III/IV)	0.982 (0.704–1.371)	0.917		NA	1.180 (0.827–1.684)	0.360		NA	1.281 (0.863–1.901)	0.219		NA
Follow-up												
Recurrence (≤2 *vs.* >2 years)	1.290 (1.057–1.574)	0.012*	1.216 (0.990–1.494)	0.063	2.232 (1.812–2.749)	<0.001*	2.182 (1.758–2.709)	<0.001*		NA		NA
VETC (absent *vs.* present)	2.218 (1.506–3.009)	<0.001*		NA	1.745 (1.213–2.510)	0.003*		NA	1.640 (1.090–2.467)	0.018*		NA
PD-L1 (low *vs.* high)	1.638 (1.188–2.258)	0.003*		NA	1.471 (1.040–2.079)	0.029*		NA	1.593 (1.079–2.353)	0.019*		NA
Intra-tumoral VETC/PD-L1 index		<0.001*		0.001*		0.003*		0.051		0.008*		0.011*
I	Ref.		Ref.		Ref.		Ref.		Ref.		Ref.	
II	0.296 (0.180–0.489)		0.356 (0.210–0.602)		0.422 (0.257–0.692)		0.552 (0.333–0.914)		0.409 (0.231–0.722)		0.422 (0.238–0.749)	
III	0.738 (0.523–1.042)		0.780 (0.541–1.124)		0.725 (0.493–1.066)		0.711 (0.480–1.053)		0.710 (0.465–1.085)		0.696 (0.453–1.069)	

*, P value showed statistical significant. CA-199, carbohydrate antigen 199; TNM, tumor-nodes-metastases; Ref., reference; HR, hazard ratio; CI, confidential interval; NA, not adopted; NS, not significant; TTR, time to relapse; OS, overall survival.

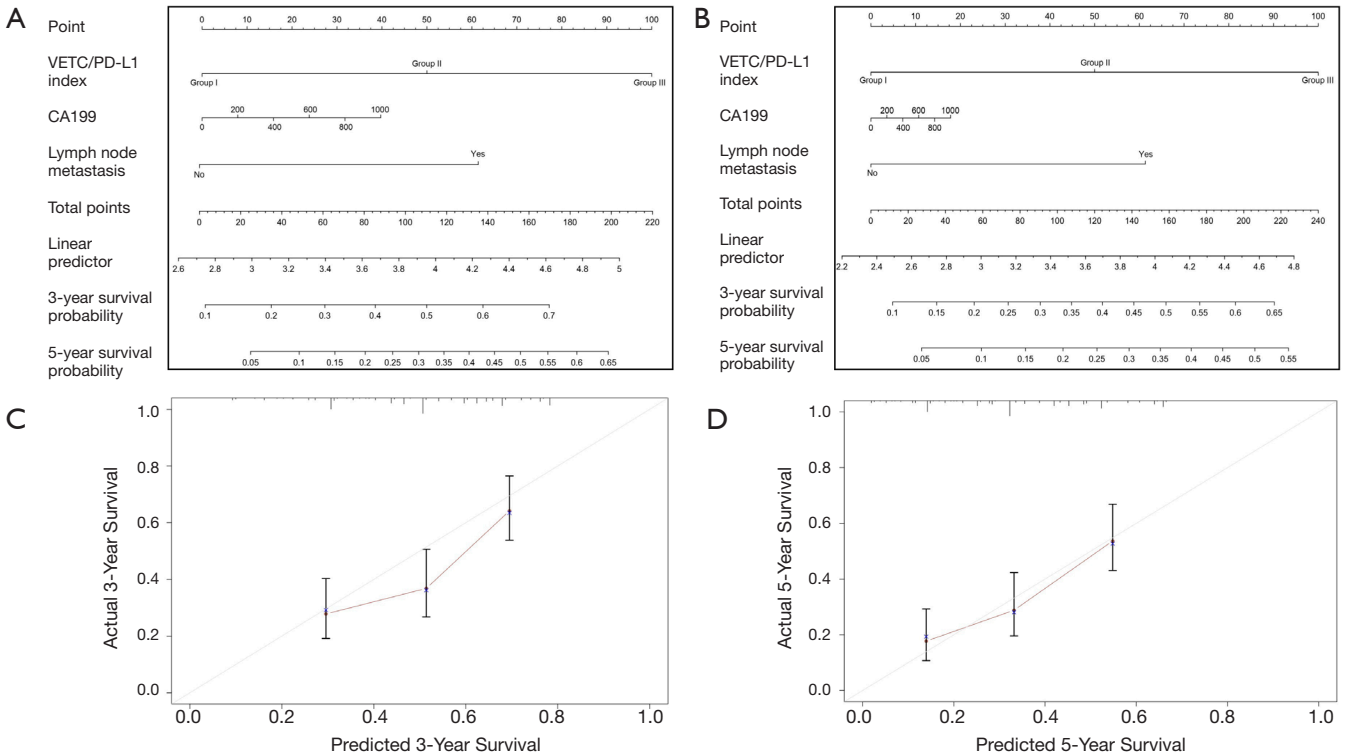

Figure 3 ICC OS nomogram and calibration curve analysis. (A,B) The ICC OS and TTR nomogram comprising CA-199, lymph node metastasis and VETC/PD-L1 index in training cohort (n=214); (C,D) The calibration curves for predicting three-year and five-year OS in training cohort (n=214). ICC, intrahepatic cholangiocarcinoma; VETC, vessels encapsulate tumor clusters; OS, overall survival.

indication for HCC patients with sorafenib applying (8). Consistently, recent studies suggest that sorafenib monotherapy may show promising anticancer activity in patients with advanced ICC with controllable toxicity (34). According to the results from the case-control study, we had shown that VETC$^+$ in ICC was ubiquitous at different clinical stages and accounted to 57.9–70%. To date, our present research was the first attempt to evaluate the clinical association of VETC phenotype in ICC. Consistent with previous studies in HCC, present study further confirmed the prognostic significance of VETC phenotype, as a robust prognostic parameter discriminating aggressive ICC. Our findings remarkably indicated that this VETC phenotype may promote malignant tumor progression of ICC.

Recently, combination therapy has made great achievements in the application of tumor therapies (35). Targeting and immunotherapy (such as PD-1 antibody) have played an essential role in HCC therapy (36). However, only about 5% of ICC patients were microsatellite unstable, which were sensitive to PD-1 antibody (37). Whether the combination therapy, such as PD-1 antibody combined with targeted drugs, can achieve the effect similar to HCC, is unknown. At present, only very preliminary, but not conclusive evidence can be found in some phase II clinical trials, and further exploration is needed.

Notably, we simultaneously evaluated the heterogeneous PD-L1 expression profile in ICC. Previously, a large cohort of epidemiological data indicated that HBV infection (38), which might result in chronic liver inflammation, immune imbalance in ICC tumorigenesis. Our results revealed that hyper-activated PD-L1 expression in intra-tumor area was positively associated with HBV infection. Furthermore, elevated PD-L1 status in intra-tumor area had dismal prognosis than those low. Our findings illustrated that the combination of amplified PD-L1 signals and HBV infection in intra-tumor areas might play an essential role in the malignant tumor progression of ICC.

Furthermore, to illustrate the clinical value of VETC/PD-L1 index, an integrated nomogram combined with VETC and PD-L1 for OS was constructed, indicating

a better prognostic performance. Values of nomograms in predicting prognosis are drawing emerging attentions in many malignancies, such as ICC (39) and HCC (40). In present research, the C-index established through our integrated nomogram was significantly better than these traditional systems, and a good concordance between predicted and observed survival probabilities was also found.

Several limitations were presented in the present research. Our findings were only made through IHC evaluations. Hence, more researches are indeed needed to uncover the potential mechanism of VETC/PD-L1 index in promoting ICC malignant progression. Moreover, the prognostic value of VETC/PD-L1 index needs further validation in prospective studies.

Understanding the key mechanisms of tumor metastasis is of great significance for tumor treatment. The comprehensive evaluation of tumor vascularization pattern, micro-environmental profile and its potential mechanisms not only offers novel ideas for the progression of anti-tumor therapy but also provides a specific theoretical basis for ICC patients. Nonetheless, further trials focused on the effects of sequential or combination therapy in ICC are warranted.

In summary, this present research illustrated that VETC$^+$ phenotype and elevated PD-L1 expression in ICC significantly associated with malignant characteristics and dismal survival. In addition, an integrated nomogram combined with VETC and PD-L1 for OS showed a better prognostic value for ICC patients than these traditional systems. The clinical significance of VETC/PD-L1 index ensured it a promising indicator of future risk stratification and customized therapy strategies.

Acknowledgments

Funding: This work was supported by grants from National Natural Science Foundation of China (81802302, 81770137, 81573423).

Footnote

Conflicts of Interest: All authors have completed the ICMJE uniform disclosure form (available at http://dx.doi.org/10.21037/tcr.2020.04.11). The authors have no conflicts of interest to declare.

Ethical Statement: The authors are accountable for all aspects of the work in ensuring that questions related to the accuracy or integrity of any part of the work are appropriately investigated and resolved. Ethical approval was obtained from the research ethics committee of Zhongshan Hospital, Fudan University, and written informed consent was obtained from each patient.

References

1. Rahnemai-Azar AA, Weisbrod AB, Dillhoff M, et al. Intrahepatic cholangiocarcinoma: current management and emerging therapies. Expert Rev Gastroenterol Hepatol 2017;11:439-49.
2. Bertuccio P, Malvezzi M, Carioli G, et al. Global trends in mortality from intrahepatic and extrahepatic cholangiocarcinoma. J Hepatol 2019;71:104-14.
3. Khan SA, Tavolari S, Brandi G. Cholangiocarcinoma: Epidemiology and risk factors. Liver Int 2019;39 Suppl 1:19-31.
4. Angelova M, Mlecnik B, Vasaturo A, et al. Evolution of Metastases in Space and Time under Immune Selection. Cell 2018;175:751-65.e16.
5. Chiang SP, Cabrera RM, Segall JE. Tumor cell intravasation. Am J Physiol Cell Physiol 2016;311:C1-C14.
6. Harney AS, Arwert EN, Entenberg D, et al. Real-Time Imaging Reveals Local, Transient Vascular Permeability, and Tumor Cell Intravasation Stimulated by TIE2hi Macrophage-Derived VEGFA. Cancer Discov 2015;5:932-43.
7. Fang JH, Zhou HC, Zhang C, et al. A novel vascular pattern promotes metastasis of hepatocellular carcinoma in an epithelial-mesenchymal transition-independent manner. Hepatology 2015;62:452-65.
8. Fang JH, Xu L, Shang LR, et al. Vessels That Encapsulate Tumor Clusters (VETC) Pattern Is a Predictor of Sorafenib Benefit in Patients with Hepatocellular Carcinoma. Hepatology 2019;70:824-39.
9. He C, Zhou Z, Jiang H, et al. Epithelial-Mesenchymal Transition is Superior to Vessels-Encapsulate Tumor Cluster in Promoting Metastasis of Hepatocellular

Carcinoma: a Morphological Evidence. J Cancer 2017;8:39-47.
10. Gide TN, Quek C, Menzies AM, et al. Distinct Immune Cell Populations Define Response to Anti-PD-1 Monotherapy and Anti-PD-1/Anti-CTLA-4 Combined Therapy. Cancer Cell 2019;35:238-55.e6.
11. Cristescu R, Mogg R, Ayers M, et al. Pan-tumor genomic biomarkers for PD-1 checkpoint blockade-based immunotherapy. Science 2018. doi: 10.1126/science.aar3593.
12. Ott PA, Bang YJ, Piha-Paul SA, et al. T-Cell-Inflamed Gene-Expression Profile, Programmed Death Ligand 1 Expression, and Tumor Mutational Burden Predict Efficacy in Patients Treated With Pembrolizumab Across 20 Cancers: KEYNOTE-028. J Clin Oncol 2019;37:318-27.
13. Ma LJ, Feng FL, Dong LQ, et al. Clinical significance of PD-1/PD-Ls gene amplification and overexpression in patients with hepatocellular carcinoma. Theranostics 2018;8:5690-702.
14. Ritprajak P, Azuma M. Intrinsic and extrinsic control of expression of the immunoregulatory molecule PD-L1 in epithelial cells and squamous cell carcinoma. Oral Oncol 2015;51:221-8.
15. Tanaka S, Kubo S. Programmed death-1 inhibitor for occupational intrahepatic cholangiocarcinoma caused by chlorinated organic solvents. J Hepatobiliary Pancreat Sci 2019;26:242-3.
16. Lu JC, Zeng HY, Sun QM, et al. Distinct PD-L1/PD1 Profiles and Clinical Implications in Intrahepatic Cholangiocarcinoma Patients with Different Risk Factors. Theranostics 2019;9:4678-87.
17. Rizvi S, Khan SA, Hallemeier CL, et al. Cholangiocarcinoma - evolving concepts and therapeutic strategies. Nat Rev Clin Oncol 2018;15:95-111.
18. Sirica AE, Gores GJ, Groopman JD, et al. Intrahepatic Cholangiocarcinoma: Continuing Challenges and Translational Advances. Hepatology 2019;69:1803-15.
19. Primrose JN, Fox RP, Palmer DH, et al. Capecitabine compared with observation in resected biliary tract cancer (BILCAP): a randomised, controlled, multicentre, phase 3 study. Lancet Oncol 2019;20:663-73.
20. Labib PL, Goodchild G, Pereira SP. Molecular Pathogenesis of Cholangiocarcinoma. BMC Cancer 2019;19:185.
21. Galon J, Bruni D. Approaches to treat immune hot, altered and cold tumours with combination immunotherapies. Nat Rev Drug Discov 2019;18:197-218.
22. Shen Y, Li S, Wang X, et al. Tumor vasculature remolding by thalidomide increases delivery and efficacy of cisplatin. J Exp Clin Cancer Res 2019;38:427.
23. Shigeta K, Datta M, Hato T, et al. Dual Programmed Death Receptor-1 and Vascular Endothelial Growth Factor Receptor-2 Blockade Promotes Vascular Normalization and Enhances Antitumor Immune Responses in Hepatocellular Carcinoma. Hepatology 2020;71:1247-61.
24. Liu LZ, Yang LX, Zheng BH, et al. CK7/CK19 index: A potential prognostic factor for postoperative intrahepatic cholangiocarcinoma patients. J Surg Oncol 2018;117:1531-9.
25. Yang LX, Gao Q, Shi JY, et al. Mitogen-activated protein kinase kinase kinase 4 deficiency in intrahepatic cholangiocarcinoma leads to invasive growth and epithelial-mesenchymal transition. Hepatology 2015;62:1804-16.
26. Deng M, Brägelmann J, Kryukov I, et al. FirebrowseR: an R client to the Broad Institute's Firehose Pipeline. Database (Oxford) 2017. doi: 10.1093/database/baw160.
27. Sakamoto Y, Kokudo N, Matsuyama Y, et al. Proposal of a new staging system for intrahepatic cholangiocarcinoma: Analysis of surgical patients from a nationwide survey of the Liver Cancer Study Group of Japan. Cancer 2016;122:61-70.
28. Wang T, Kong J, Yang X, et al. Clinical features of sarcomatoid change in patients with intrahepatic cholangiocarcinoma and prognosis after surgical liver resection: A Propensity Score Matching analysis. J Surg Oncol 2020;121:524-37.
29. Nathan H, Aloia TA, Vauthey JN, et al. A proposed staging system for intrahepatic cholangiocarcinoma. Ann Surg Oncol 2009;16:14-22.
30. Okabayashi T, Yamamoto J, Kosuge T, et al. A new staging system for mass-forming intrahepatic cholangiocarcinoma: analysis of preoperative and postoperative variables. Cancer 2001;92:2374-83.
31. Kelley RK, Bridgewater J, Gores GJ, et al. Systemic therapies for intrahepatic cholangiocarcinoma. J Hepatol 2020;72:353-63.
32. Sugino T, Yamaguchi T, Ogura G, et al. Morphological evidence for an invasion-independent metastasis pathway exists in multiple human cancers. BMC Med 2004;2:9.
33. Zhou HC, Fang JH, Shang LR, et al. MicroRNAs miR-125b and miR-100 suppress metastasis of hepatocellular carcinoma by disrupting the formation of vessels that encapsulate tumour clusters. J Pathol 2016;240:450-60.
34. Pan TT, Wang W, Jia WD, et al. A single-center

experience of sorafenib monotherapy in patients with advanced intrahepatic cholangiocarcinoma. Oncol Lett 2017;13:2957-64.
35. Colli LM, Machiela MJ, Zhang H, et al. Landscape of Combination Immunotherapy and Targeted Therapy to Improve Cancer Management. Cancer Res 2017;77:3666-71.
36. Kudo M. Targeted and immune therapies for hepatocellular carcinoma: Predictions for 2019 and beyond. World J Gastroenterol 2019;25:789-807.
37. Liu X, Yao J, Song L, et al. Local and abscopal responses in advanced intrahepatic cholangiocarcinoma with low TMB, MSS, pMMR and negative PD-L1 expression following combined therapy of SBRT with PD-1 blockade. J Immunother Cancer 2019;7:204.
38. Wang Q, Li J, Lei Z, et al. Prognosis of Intrahepatic Cholangiocarcinomas with HBV Infection is Better than Those with Hepatolithiasis After R0 Liver Resection: A Propensity Score Matching Analysis. Ann Surg Oncol 2017;24:1579-87.
39. Wang Y, Li J, Xia Y, et al. Prognostic nomogram for intrahepatic cholangiocarcinoma after partial hepatectomy. J Clin Oncol 2013;31:1188-95.
40. Chen L, Zeng F, Yao L, et al. Nomogram based on inflammatory indices for differentiating intrahepatic cholangiocarcinoma from hepatocellular carcinoma. Cancer Med 2020;9:1451-61.

Cite this article as: Tao P, Ma L, Xue R, Wang H, Zhang S. Clinicopathological and prognostic implications of vessels encapsulate tumor clusters with PD-L1 in intrahepatic cholangiocarcinoma patients. Transl Cancer Res 2020;9(5):3550-3563. doi: 10.21037/tcr.2020.04.11

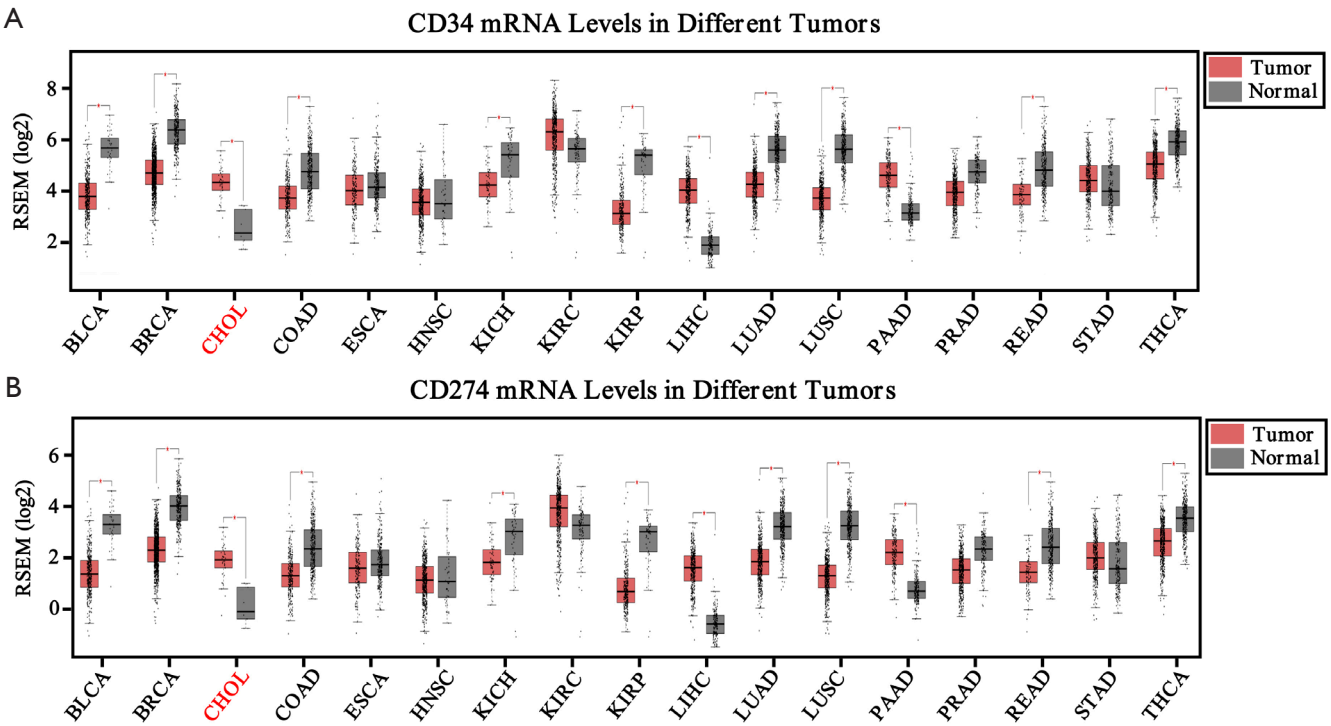

Figure S1 Transcriptome sequencing data of CD34 and PD-L1 in normal and tumor tissues from TCGA database. The mRNA level of CD34 (A) and PD-L1 (B) in pan-cancer cohort and cholangiocarcinoma (CHOL) cohort (Red) from TCGA database. BLCA, bladder urothelial Carcinoma; BRCA, breast invasive carcinoma; CHOL, cholangiocarcinoma; COAD, colon adenocarcinoma; ESCA, esophageal carcinoma; HNSC, head and neck squamous cell carcinoma; KICH, kidney chromophobe; KIRC, kidney renal clear cell carcinoma; KIRP, kidney renal papillary cell carcinoma; LIHC, liver hepatocellular carcinoma; LUAD, lung adenocarcinoma; LUSC, lung squamous cell carcinoma; PAAD, pancreatic adenocarcinoma; PRAD, prostate adenocarcinoma; READ, rectum adenocarcinoma; STAD, stomach adenocarcinoma; THCA, thyroid carcinoma.

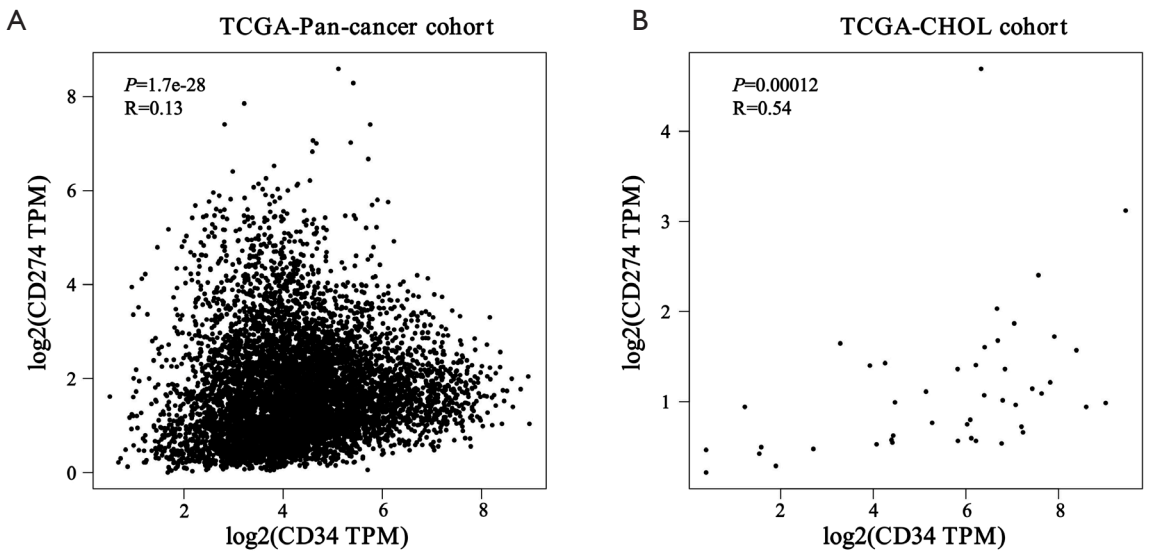

Figure S2 Correlation between CD34 and PD-L1 mRNA expression in pan-cancer cohort (A) and cholangiocarcinoma (CHOL) cohort (B).

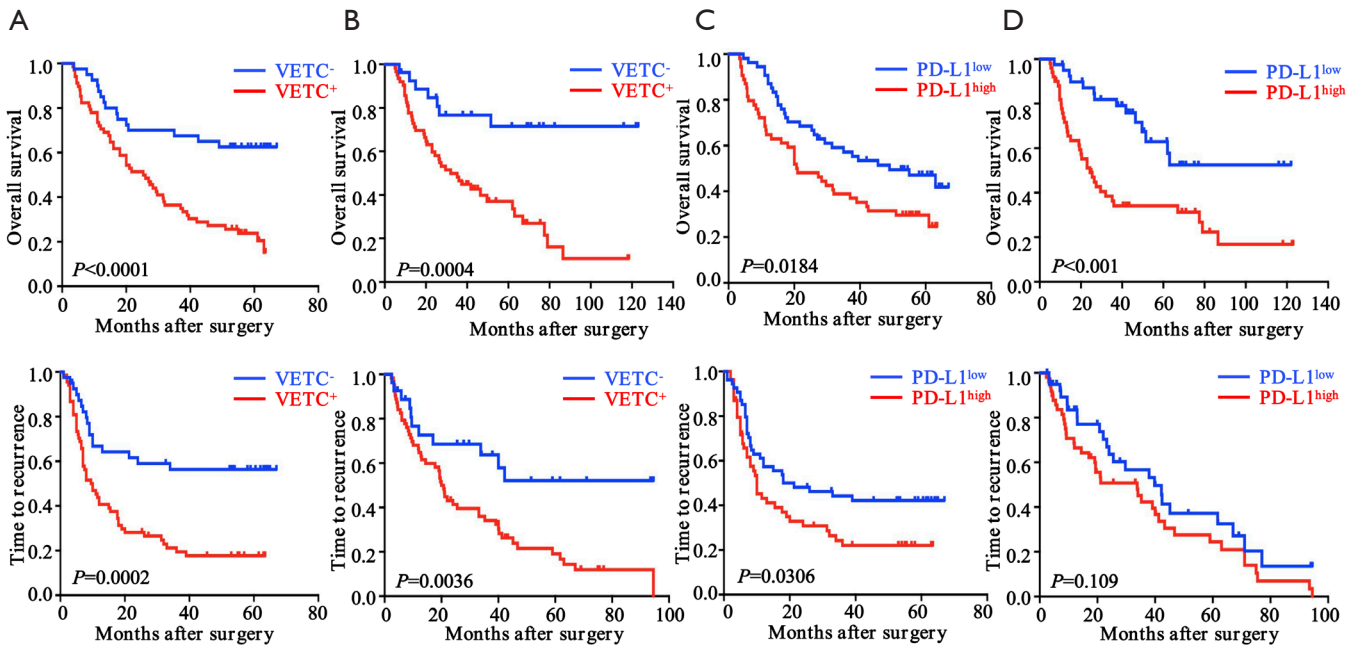

Figure S3 Clinical implications of VETC and PD-L1 in ICC in validation and external validation cohorts. (A) Kaplan-Meier curves for OS and TTR based on VETC pattern invalidation cohort (n=108); (B) Kaplan-Meier curves for OS and TTR based on VETC pattern in external validation cohort (n=90); (C) Kaplan-Meier curves for OS and TTR based on PD-L1 expression invalidation cohort (n=108); (D) Kaplan-Meier curves for OS and TTR based on PD-L1 expression in external validation cohort (n=90). VETC, vessels encapsulate tumor clusters; ICC, intrahepatic cholangiocarcinoma; TTR, time to relapse; OS, overall survival.

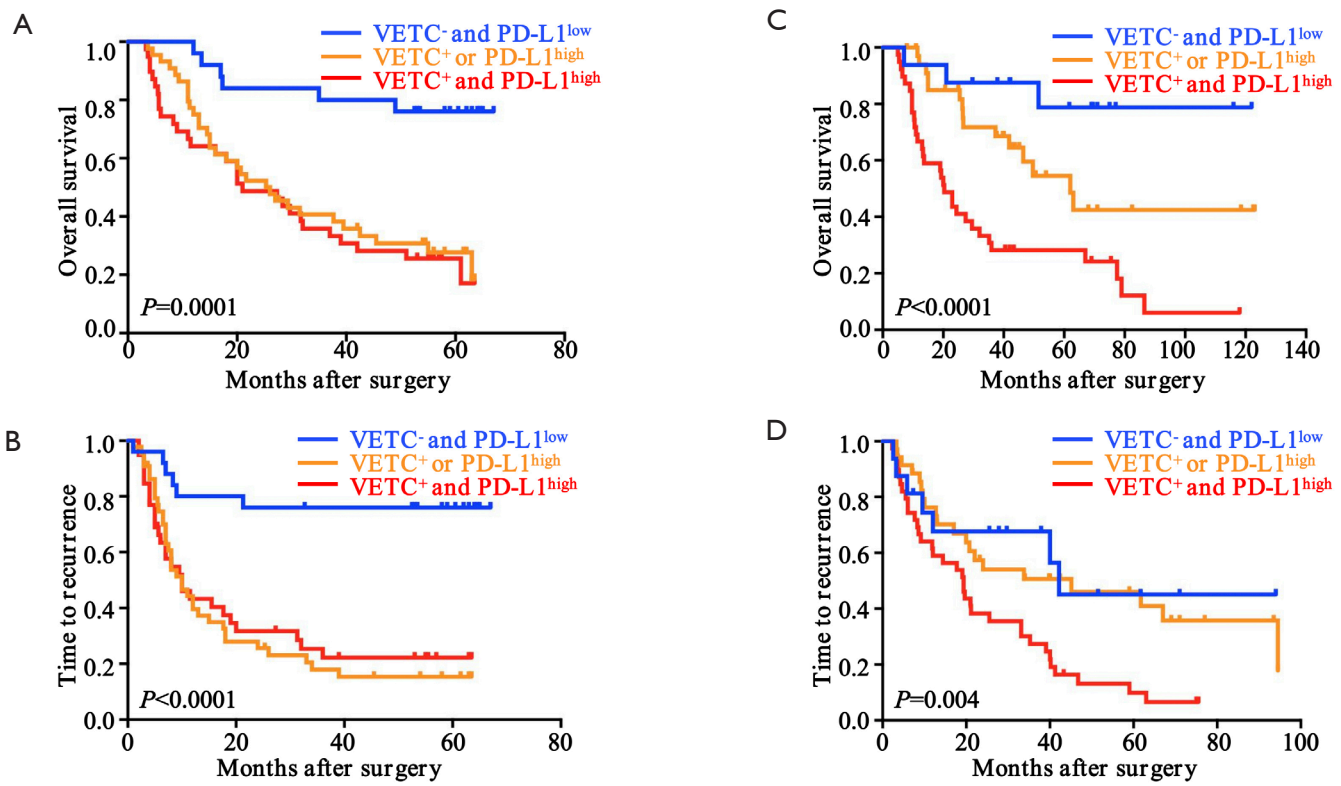

Figure S4 Clinical implications of VETC and PD-L1 in ICC. Kaplan-Meier curves for OS and TTR based on combined VETC pattern and PD-L1 expression in validation (n=108) and external validation cohorts (n=90). VETC, vessels encapsulate tumor clusters; ICC, intrahepatic cholangiocarcinoma; TTR, time to relapse; OS, overall survival.

Table S1 Impact of clinical and pathological features on OS, TTR and early recurrence in validation cohort (n=108)

Variables	OS (n=108)				TTR (n=108)				Early recurrence (n=108)			
	Univariable analysis		Multivariable analysis		Univariable analysis		Multivariable analysis		Univariable analysis		Multivariable analysis	
	HR (95% CI)	P	HR (95% CI)	P	HR (95% CI)	P	HR (95% CI)	P	HR (95% CI)	P	HR (95% CI)	P
Clinical features												
Gender (male *vs.* female)	1.266 (0.881–1.819)	0.202		NA	1.106 (0.773–1.583)	0.581		NA	1.448 (0.857–2.448)	0.166		NA
Age, median (range), years	1.026 (0.726–1.448)	0.886		NA	0.994 (0.703–1.406)	0.973		NA	0.667 (0.406–1.907)	0.111		NA
HBV infection (negative *vs.* positive)	0.751 (0.528–1.068)	0.111		NA	0.755 (0.528–1.078)	0.122		NA	1.018 (0.612–1.693)	0.945		NA
AFP (ng/mL) (<20 *vs.* ≥20)	0.628 (0.347–1.138)	0.125		NA	0.784 (0.450–1.366)	0.390		NA	0.780 (0.371–1.639)	0.513		NA
CA-199 (U/mL) (<37 *vs.* ≥37)	1.284 (0.910–1.813)	0.155		NA	1.232 (0.871–1.744)	0.238		NA	1.825 (1.112–2.996)	0.017*	1.768 (1.035–3.020)	0.037*
Lymphonodus metastasis (absent *vs.* present)	3.700 (2.468–5.547)	<0.001*	5.075 (1.383–18.616)	0.014*	3.041 (2.012–4.598)	<0.001*	3.983 (1.208–13.234)	0.023	3.890 (2.211–6.843)	<0.001*	2.893 (0.792–10.569)	0.108
TNM stage (I *vs.* II+III)	2.819 (1.929–4.120)	<0.001*	0.629 (0.185–2.136)	0.457	2.343 (1.587–3.461)	<0.001*	0.763 (0.262–2.226)	0.621	2.903 (1.710–4.926)	<0.001*	0.899 (0.266–3.040)	0.864
Child-Pugh stage (A *vs.* B)	0.694 (0.221–2.183)	0.532		NA	0.869 (0.321–2.354)	0.782		NA	5.138 (1.207–21.864)	0.027*	1.394 (0.301–6.445)	0.671
General macroscopic												
Tumor number (single *vs.* multiple)	1.846 (1.266–2.692)	0.001*	0.950 (0.541–1.669)	0.858	2.020 (1.385–2.946)	<0.001*	1.750 (1.002–3.056)	0.049*	1.986 (1.178–3.346)	0.01*	1.760 (0.978–3.167)	0.059
Tumor size (≤5 *vs.* >5)	1.735 (1.218–2.472)	0.002*	1.712 (1.029–2.847)	0.039*	1.340 (0.944–1.902)	0.101		NA	1.542 (0.937–2.536)	0.088		NA
Macrovascular invasion (absent *vs.* present)	1.212 (0.744–1.975)	0.440		NA	1.310 (0.813–2.112)	0.268		NA	0.817 (0.372–1.793)	0.614		NA
General microscopic												
Liver cirrhosis (absent *vs.* present)	1.102 (0.750–1.620)	0.620		NA	1.073 (0.725–1.590)	0.724		NA	1.152 (0.682–1.945)	0.597		NA
Tumor encapsulation (complete *vs.* none)	1.230 (0.727–2.079)	0.441		NA	1.274 (0.743–2.184)	0.379		NA	0.817 (0.443–1.505)	0.516		NA
Follow-up												
Recurrence (≤2 *vs.* >2 years)	1.939 (1.380–2.723)	<0.001*	1.407 (0.914–2.166)	0.121	2.793 (2.044–3.816)	<0.001*	2.513 (1.713–3.686)	<0.001*		NA		NA
VETC (absent *vs.* present)	2.064 (1.428–2.982)	<0.001*			1.899 (1.318–2.734)	0.001*			2.368 (1.339–4.188)	0.003*		
PD-L1 (low *vs.* high)	2.096 (1.466–2.997)	<0.001*			1.750 (1.229–2.493)	0.002*			1.591 (0.966–2.618)	0.068		
Intratumoral VETC/PD-L1 index		<0.001*		0.023*		<0.001*		0.111		0.003*		0.002
I	Ref.		Ref.		Ref.		Ref.		Ref.		Ref.	
II	0.201 (0.109–0.372)		0.265 (0.101–0.700)		0.261 (0.145–0.469)		0.431 (0.163–1.142)		0.233 (0.095–0.570)		0.261 (0.106–0.644)	
III	0.755 (0.496–1.149)		0.924 (0.556–1.595)		0.782 (0.508–1.204)		1.206 (0.716–2.031)		1.058 (0.627–1.786)		1.370 (0.775–2.420)	

*, P value showed statistical significant. CA-199, carbohydrate antigen 199; TNM, tumor-nodes-metastases; Ref., reference; HR, hazard ratio; CI, confidential interval; NA, not adopted; NS, not significant; TTR, time to relapse; OS, overall survival.

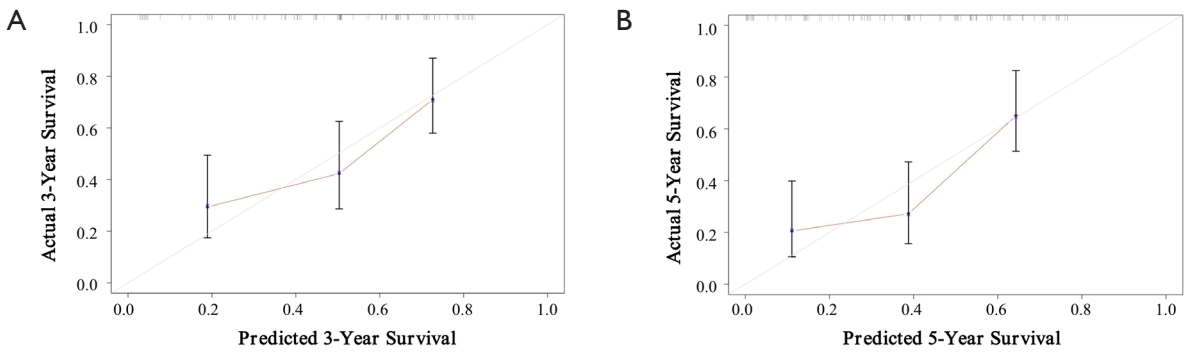

Figure S5 ICC OS nomogram and calibration curve analysis. The calibration curves for predicting 3-year (A) and 5-year (B) OS in validation cohort (n=108). ICC, intrahepatic cholangiocarcinoma; OS, overall survival.